PAR reduction revisited: an extension to Tellado's method

Werner Henkel and Valentin Zrno
Telecommunications Research Center Vienna (FTW)
Vienna, Austria
Werner.Henkel@ieee.org

Abstract—**Multi-tone modulation (DMT, Discrete Multitone, OFDM, Orthogonal Frequency Division Multiplex) has the disadvantage of a high peak-to-average ratio (PAR). The least complex approach for peak reduction by Jose Tellado called 'tone reservation', operating completely in time domain, has not been able to take into account the transmit filter, which increases the PAR, again, due to overshooting. Herein, we propose an extended procedure that is able to account for any arbitrary filter response.**

Keywords— **PAR, peak-to-average ratio, Crest factor, DMT, OFDM**

I. Tellado's tone reservation method

Tellado's original procedure reduces peaks in the time domain by iterative subtraction of Dirac-like functions. The idea is developed from the finding that clipped portions of the time-domain signal can be written as

$$\mathbf{x} - \mathbf{x}_{clip} = \sum_i \beta_i \cdot (\delta \to m_i) \ , \qquad (1)$$

where the β_i are the values exceeding the clip threshold $\mathbf{x}_{clip}$ and the m_i are the clip locations. "$\to m$" denotes (cyclic) shift by m and δ is the Dirac vector with a one at time zero and zero elsewhere. The Dirac function δ would require the whole DFT frame and would thus not allow to transmit information any more. The idea is now to reserve only some of the frequency bins and use them to generate a Dirac-like time-domain signal $\mathbf{p}$ that could be subtracted iteratively (at peak locations) from the signal resulting from the remaining carriers[1] used for arbitrary data. This means that (1) is approximated by

$$\sum_i \beta_i \cdot (\delta \to m_i) \approx \sum_i \gamma_i \cdot (\mathbf{p} \to m_i) \ , \qquad (2)$$

with some weighting coefficients γ_i. A simplistic approach to find a suitable Dirac-like function $\mathbf{p}$ is to set all reserved carriers (DFT bins) to a constant (such that a Dirac-like function with its maximum normalized to unity is obtained). If the bins are chosen at random, after a certain number of trials, one is able to find a set of such bins that shows a sufficient peak compared to the sidelobes in the corresponding time-domain vector. Additionally to choosing bins at random, some fixed positions may be selected which are not used for data transmission at all or where the signal-to-noise ratio is low. An example Dirac-like function is shown in Fig. 1 which has been produced with 5% randomly chosen frequency bins. (This percentage of 5% is used throughout for all examples.)

After having selected the bins and stored the corresponding time-domain vector, the following algorithm is applied:

1. Initialize $\mathbf{X}$ to be the DFT-domain information vector with reserved carriers set to zero.
2. Initialize the time domain solution $\mathbf{x}^{(0)}$ to $\mathbf{x}$, which results from the IFFT($\mathbf{X}$).
3. Find the value $x_m^{(i)}$ and location m for which $|x_m^{(i)}| = \max_k |x_k^{(i)}|$
4. If $|x_m^{(i)}| < x_{target}$ of if $i > i_{max}$ then stop the iteration and transmit $\mathbf{x}^{(i)}$, otherwise
5. Update the time-domain vector according to

$$\mathbf{x}^{(i+1)} = \mathbf{x}^{(i)} - \alpha \cdot (x_m^{(i)} - \text{sign}(x_m^{(i)}) \cdot x_{target}) \cdot (\mathbf{p} \to m) \qquad (3)$$

$i := i + 1$;
goto 3.

Equation (3) is a simplification of a gradient method consisting of multiple reductions in one step. The term $\alpha \cdot (x_m^{(i)} - \text{sign}(x_m^{(i)}) \cdot x_{target})$ results in a possible realization of the γ_i in (2). As in similar gradient procedures, α determines the step size and should be chosen dependent on x_{target} which denotes the desired maximum value. This is the threshold that should not be exceeded. The iterative reduction procedure tries to force such exceeding values to below the threshold.[2]

[1] At the receiver, only these carriers are evaluated.

[2] We determine this threshold by a desired PAR limit per time-domain block. This results in a threshold that varies from block to

α should grow with the PAR limit. High values of the step size α result in worse convergence, since sidelobes of the impulse-like vector p can more easily cause new peaks exceeding the relatively low threshold at other locations. The further the threshold is from the RMS value, the lower the chance is to generate a new value exceeding the threshold elsewhere.

Figures 2 and 3 show the complementary cumulative frequency distribution, i.e., the probabilities of exceeding a given PAR[3] and the corresponding voltage histogram, respectively.

II. THE EXTENSION

Tellado already reported drastic performance degradations when evaluating the PAR after the transmit filter, which is the point of interest when the filtering is done before the line driver. He also reported in [4] that the "structure of the FFT operator is lost after filtering" which we interpret as a statement that no suitable procedure had been found that could take the filter properties into account and maintain the performance of the procedure.

Nevertheless, we found that introducing the filter response into the procedure is possible. To this end we use an oversampling by, e.g., $L = 4$ to represent the analog waveform with sufficient accuracy. Then, we determine a random placement of reserved carriers that result in a Dirac-like function after upsampling and filtering. This may not result in a nicely shaped Dirac-like impulse shape at the input of the filter. This property is however not required there, but at the output of the filter. In the oversampled domain, we define not only one, but L Dirac-like functions and try to space them by one sample. The shift in the oversampled signal is realized by the (circular) time shift property of the DFT transform

$$x(n - l \bmod (LN)) \circ\!\!-\!\!\bullet X(k) e^{-jkl\frac{2\pi}{LN}} \ . \qquad (4)$$

This shift property, i.e., the rotation by $-jkl\frac{2\pi}{LN}$, is applied only to those components which correspond to the original (non-oversampled) DFT frame. Through an IFFT with the original (non-oversampled) blocksize, we obtain L non-oversampled time-domain vectors. In parallel, an oversampled filtered Dirac-like vector set is generated thus leading to two sets of "Dirac-like" vectors, before and after oversampling, with L vectors, each. Figure 4 shows the corresponding block diagram. The uppermost blocks locate the peak of the oversampled Dirac-like function. The subsequent block with rounded edges realizes a time shift to zero and the neighboring $L-1$ positions. This is done applying the shift property to the reserved carriers. The shift to zero is required, since an arbitrary filter response will also place the peak of the Dirac-like function to some arbitrary position. The division by $1/|\tilde{p}_m|$ normalizes the peak to unity.

For actual peak reduction (see, Fig. 5), one of the L vectors with the desired peak location (at the cancellation position) is selected in the oversampled domain and in parallel, the same selection and updating operation is performed with the corresponding vectors before oversampling. This procedure generates a time-domain signal in the original sampling rate that can then be fed into the real existing filter. The upper part of Fig. 5 shows the processing of the non-oversampled signal, whereas the lower part shows the parallel operations in oversampled mode. For iterative subtraction, the necessary shift is split into a shift in the original non-oversampled spacing $\lfloor m/L \rfloor$ and the remaining shift of a fraction of the original spacing is realized by the choice within the set of L functions (index $(m \bmod L)$).
The resulting oversampled signal $\tilde{\mathbf{x}}$ at the end of the iterations after the stop condition has been reached is usually not required, since the non-oversampled signal is to be fed through the real existing filter. Note that the iterative procedure is controlled by the oversampled filtered signal and the non-oversampled is just computed together with it. As output, however, the non-oversampled and not filtered signal is required. The iterations are terminated when all samples' absolute values fall below the target level x_{target} or the maximum number of iterations i_{max} has been reached.

We will study two different filter responses: a rectangular response which limits the band to exactly half of the original sampling frequency ($1/(2L)$ of the oversampled one), and a Butterworth filter response chosen similar to the definition in the ITU-T G.996.1 standards document stating a typical ADSL roll-off (additionally, $\sin(x)/x$-roll-off from sample and hold),

$$F_{BW}(j\omega) = \frac{1}{\prod_{n=0}^{n=\alpha/2-1}\left(\frac{j\omega}{s_n} - 1\right)} \ , \qquad (5)$$

$$\text{with } s_n = \omega_{3\text{dB}} \cdot e^{j\pi\left(\frac{1}{2} + \frac{1+2n}{\alpha}\right)} \ ,$$

where $\omega_{3\text{dB}}$ denotes the 3-dB edge frequency. The order

block. This non-constant threshold also reduces smaller peaks, if the momentary average power is lower.

[3] the PAR definition in here and also presumedly in Tellado's papers uses the average power of an unprocessed signal (with all carriers assumed to be active except for the unprocessed reference curve where the reserved carriers have been set to zero) as reference and is thus a direct measure for the peak voltage.

$\alpha/2$ is selected to be 6. The corresponding amplitude response (squared) is

$$|F_{BW}(j\omega)|^2 = \frac{1}{1+\left(\frac{\omega}{\omega_{3\text{dB}}}\right)^{\alpha}} \; . \qquad (6)$$

Together with the $\sin(x)/x$-roll-off, we obtain from (5)

$$F_{BW}(j\omega) = \frac{1}{\prod_{n=0}^{n=\alpha/2-1}\left(\frac{j\omega}{s_n}-1\right)} \cdot \frac{\sin(\omega T_s/2)}{\omega T_s/2} \; , \qquad (7)$$

with T_s the sampling rate (2.208 MHz for ADSL).

The Butterworth filter does not strictly limit the band according to the sampling theorem. As has been stated in (4), a time-shift results in a rotation in the DFT domain, if we consider extended vectors according to the oversampling. A phase rotation in the non-extended DFT-domain vector cannot represent rotations in alias bands. This causes differences in the shape of the L shifted versions of the Dirac-like functions. The ensembles of four ($L = 4$) Dirac-like functions at the output of the rectangular and the Butterworth filters are shown in figures 6 and 7, respectively. The impulses at the output of the Butterworth filter do not always show the desired optimum locations of the peaks (aliasing). This may be controlled by modifying the rotation.

The corresponding vectors at the input of the filters (not shown) are even further from the equidistant spacing. However, the Dirac-like properties and right positions are required for the output of the filter, not for the input.

III. Performance results

We compare the results of our new approach to the original non-oversampled Tellado method. In all cases, the performance at the output of the transmit filter is investigated. Figure 8 shows the convergence in steps of 10 iterations of the new approach dependent on the target PAR and the step size. Figure 9 compares the complementary cumulative frequency distributions over the PAR, i.e., the probabilities of exceeding a given PAR, and Fig. 10 compares the corresponding different histograms using 40 iterations for the new algorithm. The limiting effect of the procedure is clearly visible and also the dependency on the target PAR and on the step size. The results show that the performance of the new extended method does not seem to depend much on the actual shape of the transmit filter's frequency response. This is in contrast to the original approach, where especially steep filter slopes like that of the brick-wall filter lead to weak performances. Compared to the filtered original approach, we obtain PAR gains (at 10^{-5}) of 3.3 dB and 1.9 dB for the rectangular and the Butterworth filters, respectively, and we are only 0.6 dB off the performance of the unfiltered original approach (which cannot be achieved in reality).

IV. Conclusions

We have described an extension to the peak-power reduction scheme originally proposed by Tellado. The method is based on precomputing two sets of time-domain vectors *before and after the transmit filter*. The ones after the transmit filter have single spikes at neighboring positions. These Dirac-like vectors are generated by reserved carriers and are used to reducte the peak values by iterative subtraction. In order to determine the oversampled time-domain signal, a larger FFT size is required, which determined the complexity. The procedure proved to deliver significant PAR reduction gains almost independent of the actual filter response.

Acknowledgement

The authors would like to thank Jossy Sayir for his thorough reading and valuable comments.

References

[1] **Tellado, J., Cioffi, J.M.**, "PAR Reduction in Multicarrier Transmission Systems", *Delayed Contribution ITU-T 4/15*, D.150 (WP 1/15), Geneva, February 9-20, 1998.

[2] **Tellado, J., Cioffi, J.M.**, "Peak Power Reduction for Multicarrier Transmission", *Globecom '99*, Rio de Janeiro, Brazil, Dec. 5-9, 1999.

[3] **Tellado, J., Cioffi, J.M.**, "PAR Reduction with Minimal or Zero Bandwidth Loss and Low Complexity", *Contribution T1E1.4*, 98-173, June 1-5, 1998.

[4] **Tellado, J., Cioffi, J.M.**, "Further Results on Peak-to-Average Ratio Reduction", *Contribution T1E1.4*, 98-252, Aug. 31, 1998.

[5] **Tellado, J.**, "Peak-to-Average Power Reduction for Multicarrier Modulation", *Ph.D. thesis*, Stanford University, Sept. 1999.

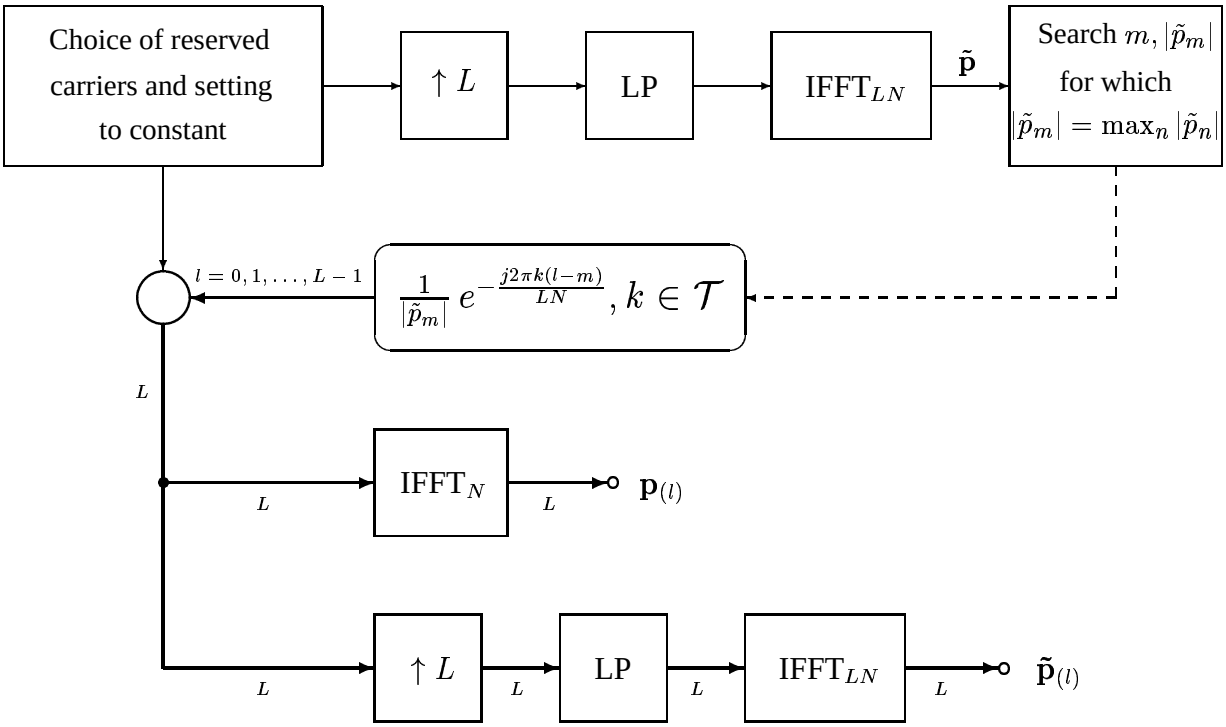

Fig. 4. Procedure for producing the two sets of Dirac-like functions ($\mathcal{T}$ denotes the set of reserved carriers.)

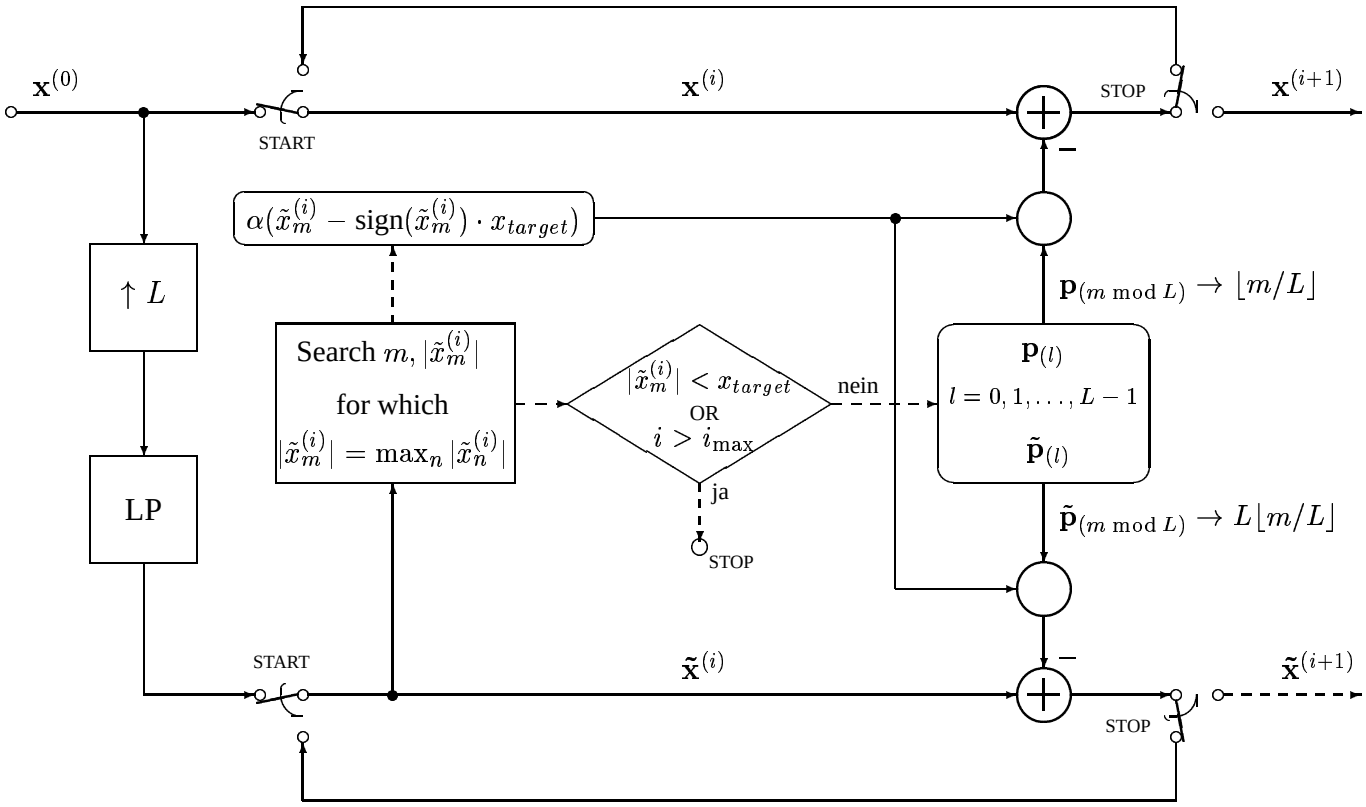

Fig. 5. Procedure for peak reduction by iterative subtraction of dirac-like function in oversampled and non-oversampled domain

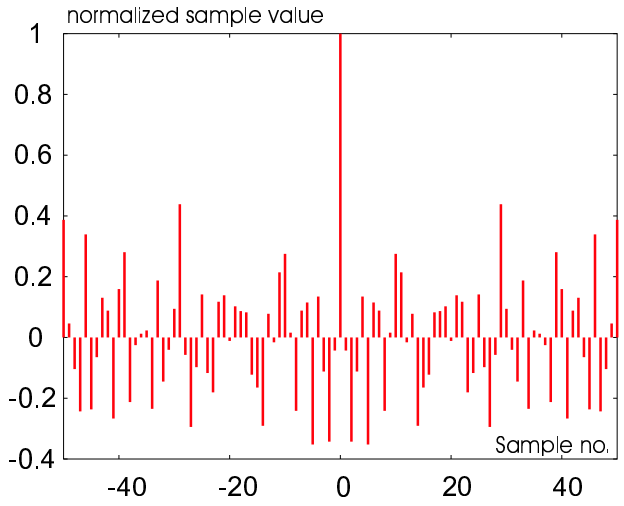

Fig. 1. Central section of a Dirac-like time-domain vector of Tellado's original procedure

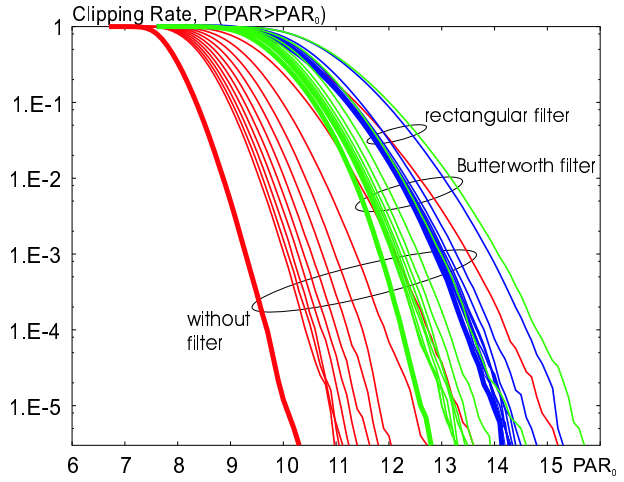

Fig. 2. Complementary cumulative frequency distributions over the PAR for Tellado's original procedure before and after filtering; convergence with first 10 iterations and the 40th (thicker)

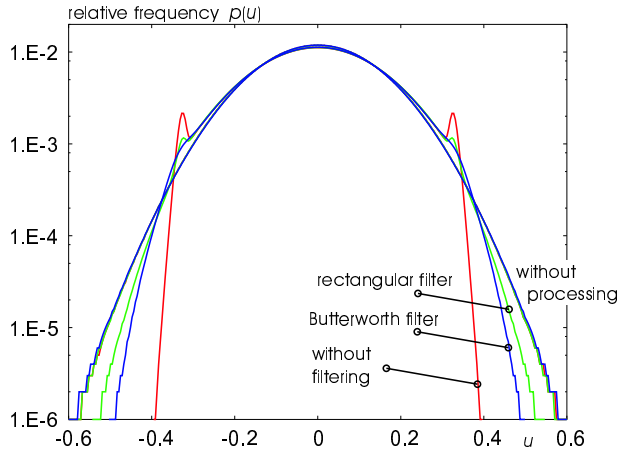

Fig. 3. Histogram of voltage samples applying Tellado's original procedure before and after filtering ($\mathcal{T}$ denotes the set of reserved carriers)

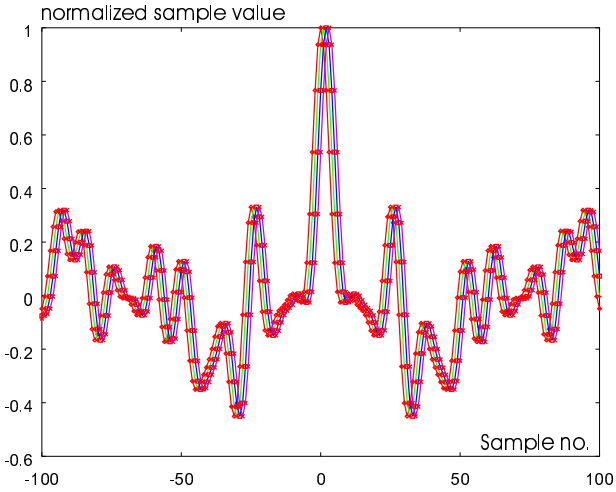

Fig. 6. Central section of a Dirac-like function at the output of a brick-wall filter

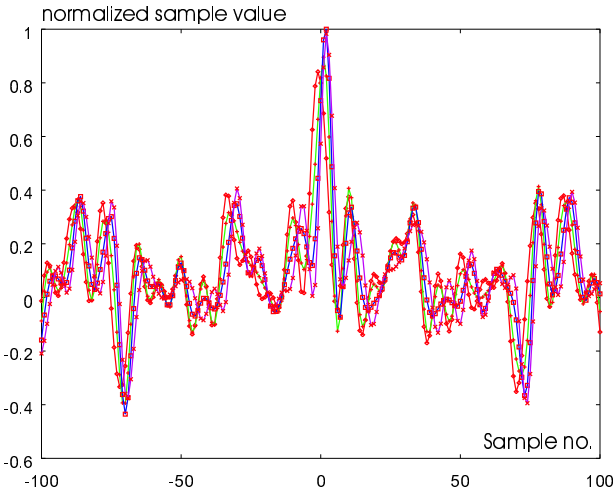

Fig. 7. Central section of a Dirac-like function at the output of a Butterworth filter

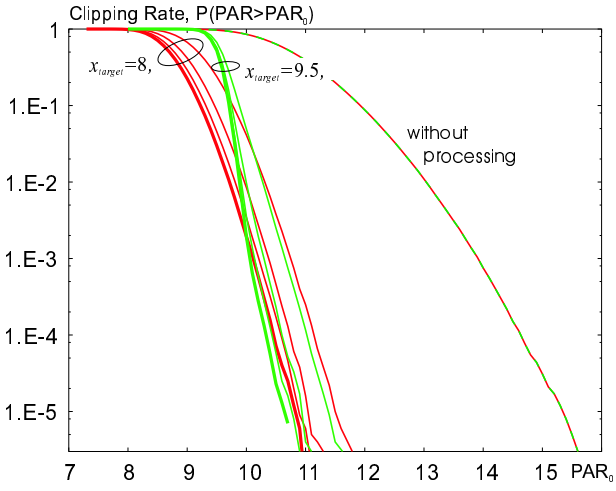

Fig. 8. Convergence of the new extended procedure in steps of 10 iterations (40th iteration thicker)

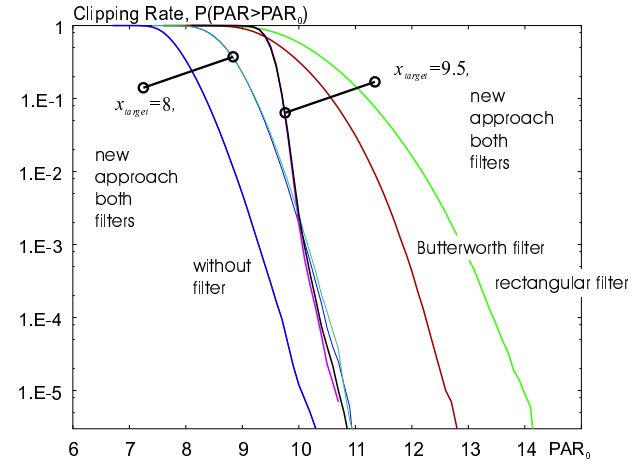

Fig. 9. Comparison of the complementary cumulative frequency distributions over the PAR of the new extended procedure (40 iterations) in relation to Tellado's original approach

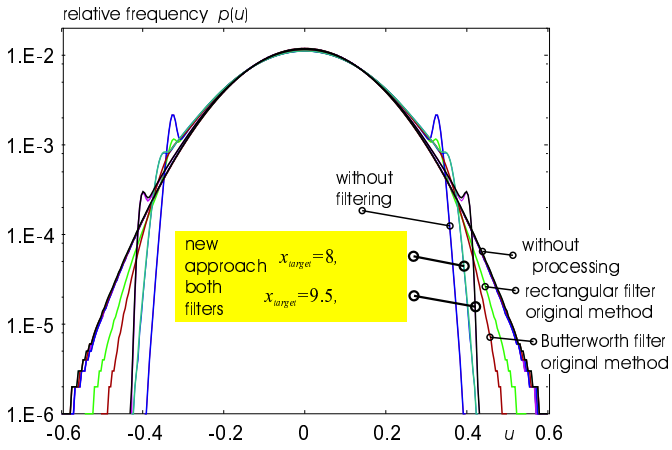

Fig. 10. Comparison of histograms of the new extended procedure (40 iterations) with Tellado's original approach